

Reconstruction of sound speed profile through natural generalized inverse technique

T V Ramana Murty, Y K Somayajulu & C S Murty

National Institute of Oceanography, Dona Paula, Goa-403 004, India

Received 14 August 1995, revised 1 February 1996

An acoustic model has been developed for reconstruction of vertical sound speed in a near stable or stratified ocean. Generalized inverse method is utilised in the model development. Numerical experiments have been carried out to account for the noise while reconstructing the model parameters. The results (data kernel, generalized inverse operator, model parameter resolution, data resolution etc.) obtained thereof have been presented.

During the late seventies, to probe the interior of the ocean, Munk & Wunsch¹ advanced a method known as ocean acoustic tomography—which takes advantage of the principle of transparency of sound waves in the ocean—for mapping the ocean interior layer by layer. The variations in travel time of acoustic pulses from acoustic source(s) to receiver(s) placed on moorings in the sea are measured. These variations reflect the changing sound speed (or temperature) field of the medium of propagation. Use of algorithms appropriate to transform the observed acoustic travel time data enables reconstruction of three-dimensional images of the sound speed field².

The numerical methods used in the formulation of the forward and inverse problems of ocean acoustic tomography have been detailed elsewhere^{3,4}. In the present study the application of generalized inverse technique^{5,6} through model simulation to the region of Arabian Sea is addressed. When estimating the model perturbation using SVD, one needs to consider the contribution of dynamic noise due to source-receiver displacements on the mooring line(s) both in the horizontal and vertical directions during transmissions.

Materials and Methods

Inverse problem—The relationship between the travel time of an acoustic pulse and the distribution of sound speed¹ can be written as

$$t(x_s, x_r, C) = \int_{\Gamma_i} \frac{ds}{C(\underline{x})} \quad \dots \quad (1)$$

where Γ_i is the ray path, x_s is the source location, and x_r is the receiver location. One may linearize

the model of the sound speed field $C(\underline{x})$ by expressing

$$C(x, y, z, t) = C_0(z) + \delta C(x, y, z) + \Delta C(x, y, z, t) \quad \dots \quad (2)$$

where the terms on the right side represent the mean reference sound speed, the effects due to mesoscale eddies and fronts, the random fluctuations due to the internal wave phenomena, small scale turbulence etc. Neglecting random fluctuations, the first order equation takes the form

$$\delta t_i = - \int_{\Gamma_{i0}} \frac{\delta C(\underline{x})}{C_0^2(\underline{x})} ds + 0 \quad (\delta C^2) \quad \dots \quad (3)$$

Here, the travel-time deviations (δt) are linearly related to the sound speed deviations for small sound speed perturbations $\delta C(\underline{x})$. In the matrix notation eqn (3) takes the form

$$\Delta \delta C = \delta T; \quad \delta C = \{\delta C_j\}; \quad \delta T = \{\delta T_i\} \quad \dots \quad (4)$$

which is solved by using generalised inverse method through SVD to obtain the following solution

$$\delta C_p = VV^T \delta C = A_g^{-1} \delta T \quad \dots \quad (5)$$

where $A_g^{-1} = V\Gamma^{-1}U^T$ is the natural generalised inverse operator, U and V are orthogonal matrices and Γ is the diagonal matrix containing the eigen values (1_i^2) arranged in the decreasing order. Once the solution is obtained, it is necessary to assess how well the data determines the model parameters. This is done through model resolution ($V_p V_p^T$) and data resolution ($U_p U_p^T$) matrices where p represents the number of factors.

Closeness ratio—The ratio between the sum of the factor model and that of the data matrix is

considered as the measure of closeness of the model data.

$$\text{Measure of closeness} = \frac{\sum_{i=1}^k l_i^2}{\sum_{i=1}^p l_i^2} \quad \dots (6)$$

where k is the number of factors. The first eigen function associated with the largest eigen value represents the broader features in the data (in the least square sense), while the second function and so on describe the residual mean square data. The closeness ratio is expressed in percentage in order to enable one to judge the contribution of different modes and thereby reproduce the model profile.

Travel time corrections—Two types of errors prevail in the measurement of acoustic ray arrival times, one due to the movement of the source(s) and receiver(s) on the moorings and the other caused by the drift between source and receiver clocks.

Mooring position keeping—Changes in the source receiver positions over 25 meters must be accurately known so that travel times can be corrected. During transmissions these positions can be precisely monitored through acoustic tracking of moorings with the bottom-mounted transponders, interrogated periodically. Deployment of stiff moorings, though massive and expensive, would also reduce mooring excursions to within tolerable limits. Travel time errors due to mooring motion are presented in the work of Cornuelle².

Time keeping—In a tomography experiment, the clock error must be less than about 25 ms per year. Mathematical expressions for clock error are given by Cornuelle².

Data source

The historic oceanographic data for the Arabian Sea (Fig. 1) available from the published work of Colburn⁷ are used in this study. Colburn's analysis covered the western Indian Ocean, in which the region is divided into a number of geographic areas (grids) based on climatic variability of parameters. The annual and winter mean profiles of temperature and salinity have been used to construct the mean sound speed profiles employing the empirical equations of Chen & Millero⁸. The annual and winter mean sound speed profiles are used for carrying ray trace analysis.

Results and Discussion

Computation of data kernel—Using the annual

mean and winter mean sound speed profiles, seventeen eigen rays (rays connecting a given source and receiver) have been identified³ for inversion analysis. The vertical water column has been divided into six layers viz., 0-400 m, 400-800 m, 800-1200 m, 1200-2000 m, 2000-3000 m and 3000-4000 m. For the reference sound speed profile (Fig. 2), ray path lengths in six tomography layers have been estimated to form the data kernel. An eigen ray plot for a source and receiver located at 1750 m and 1800 m respectively assuming a uniform water depth of 4000 m over the 300 km range is shown in Fig. 3. The acoustic rays scan the vertical water column between 180 m (upper limit) and 3300 m (lower limit). In this study, the refracted rays alone are used in the analysis as the reflected rays undergo significant intensity losses due to multiple bottom reflections.

The distribution of row vectors of model space (V_p) with varying energetic modes is depicted in Fig. 4 while the coverage of the column vectors of data space (U_p) for various modes (p) is presented in Fig. 5. The first eigenvector in Fig. 4 has its largest contribution of 77.58% among all eigenvectors calculated statistically, using closeness ratio approach⁴. Individual estimates of each component (layers as well as ray) are also estimated statistically. A good coverage of eigen rays in layer four contributed to 44.43% of 77.58% information in the first eigenvector (in the model space). On the other hand, in layer four, though all the eigen rays provide the information for the first eigenvector (in the data space), the contribution of flat angle rays

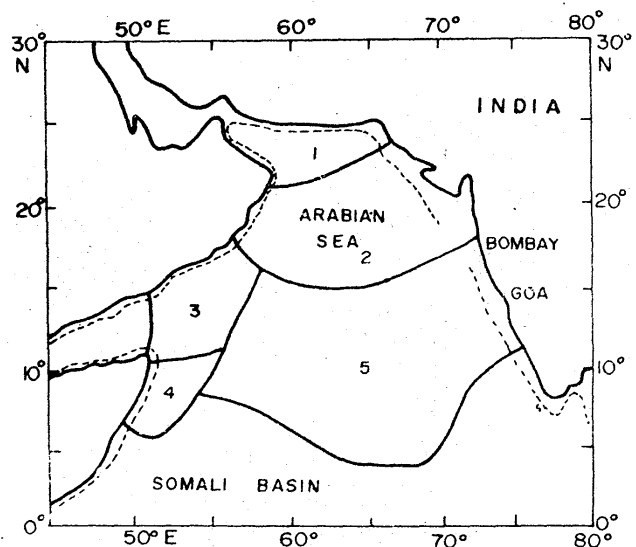


Fig. 1—Study area in the Arabian Sea

(Fig. 5a) alone is about 34.60%. This is the characteristic of the Arabian Sea where the sound speed gradients in the vicinity of the SOFAR axis are weak resulting in a large scanning depths by the flat angle rays.

The second eigenvector accounts to 17.38% of the total information resulting from contribution of three different groups of rays (Fig. 5b) viz., (a)

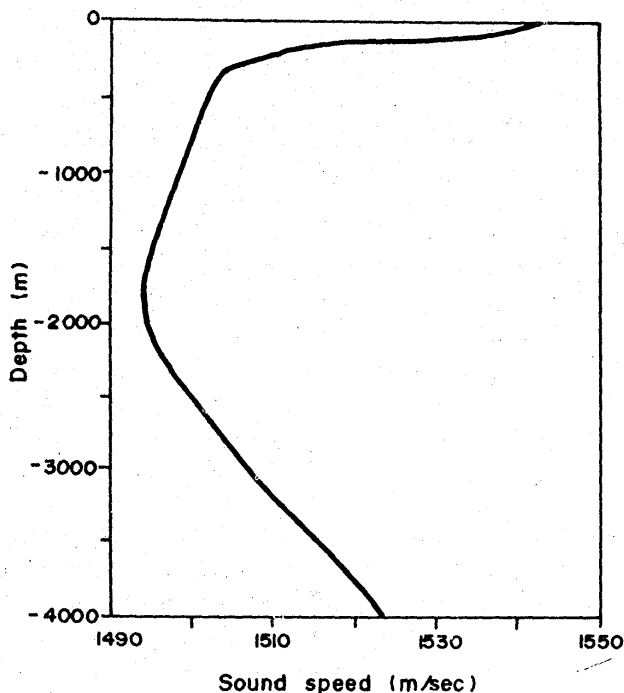


Fig. 2—Reference sound speed profile for the region

positive rays with steep angles, (b) flat angle rays (positive or negative) and (c) steep negative rays. The rays belonging to groups 1 and 3 together contribute to 33.72% in one direction while the group 2 rays account to 16.05% in the opposite direction, thus the resulting imbalance leads to a net effect of 17.54% dominated by the steep rays which is seen in all the layers other than layer four.

Coming to the higher order eigenvectors (modes 3 to 5), the coverage of the vertical water column in different layers is dominated by group 1 and 3 rays. The ray groups further split into subgroups, some being independent while the other dependent. This is due to decay in amplitudes of group 2 rays in layers 3 to 5 which imbalance groups 1 and 3 rays.

In the present analysis, the percentage of contribution of the 6th eigenvector, calculated using eqn. (6), comes to around 0.14%. By considering all the six modes for constructing the generalized inverse operator to obtain the solution, the noise in the data kernel prevailing in the form of small eigenvalues increases the rank of the matrix apart from amplifying the solution since the eigen values are present in the denominator of eqn. (5).

To construct the natural generalized inverse operator, it is essential to remove the noise present in the original data kernel (A). This can be done by approximating the data kernel by the filtered kernel⁹. The vertical distribution of the original data kernel (A) is shown in Fig. 6a. The contour pattern in this diagram indicates maximum anomaly in the

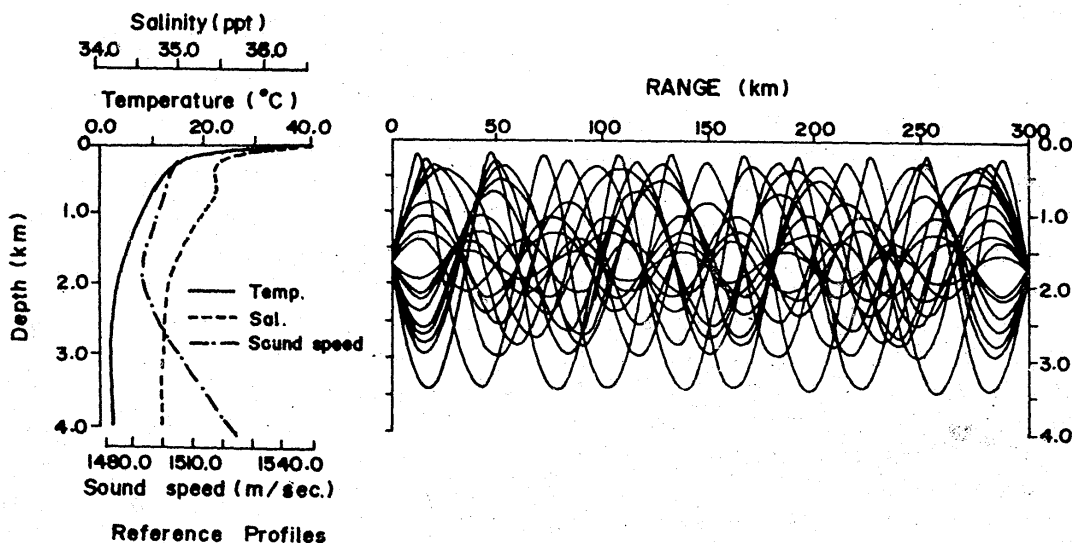


Fig. 3—Eigen ray plot between hypothetical source and receiver separated by a range 300 km

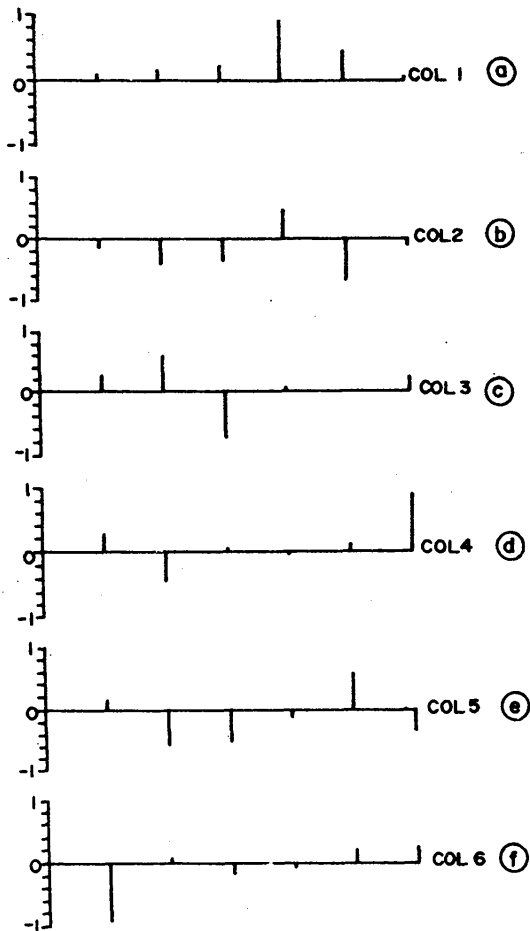


Fig. 4—Column vectors of V_p versus mode amplitude with varying energetic modes (p)

vicinity of the sound speed minimum layer. This is due to the nature of the SOFAR channel where ray bending takes place towards the sound speed minimum forming an envelope. Figure 6b presents the filtered data kernel obtained through reconstruction using five energetic modes belonging to the activated spaces of model and data matrices after removing the noise vector. This represents rich-information of the original signal of the data kernel (A). Both the plots are close to each other indicating that the information contained by many rays (Fig. 6a) can be expressed in terms of a few modes. Thus, in the case of the waters of the Arabian Sea, it is sufficient to consider six layers and five energetic modes for the construction of generalized inverse operator (Fig. 6c) that operates on travel time perturbation (δT_i) for predicting the model parameter.

Travel time data—The predicted travel times of eigen rays (say T_{pre}) computed using the mean sound speed profile reference state and the ones

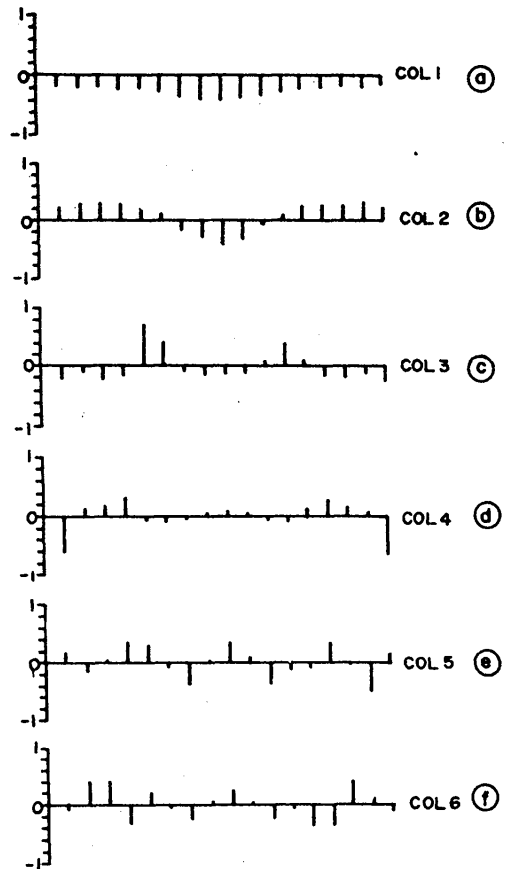


Fig. 5—Column vectors of U_p versus mode amplitude with varying energetic modes (p)

obtained for the assumed profile (winter season mean) have been used to generate possible perturbations in travel times (T_{obs}) which show variations between 0.7 and 117 ms. These travel time perturbations are operated by the generalized inverse operator (Fig. 6c) to get the model parameter perturbation (δC) in different layers (Fig. 7).

The travel time data discussed above is noise free in nature representing ideal case. In real cases, errors in travel time measurements prevail due to the dynamics of the medium as said in the previous section.

Model parameter perturbations—The assumed and reconstructed perturbations of sound speed for different eigen modes are presented in Table 1 (columns 4, 6) for comparison and are also depicted in Fig. 7 in the form of a scatter diagram. The results indicate that for a six layer model, the first five eigenvectors can reproduce the features adequately but when all the six modes are used, the sixth mode deteriorated the accuracy of the solution (Table 1, col. 7).

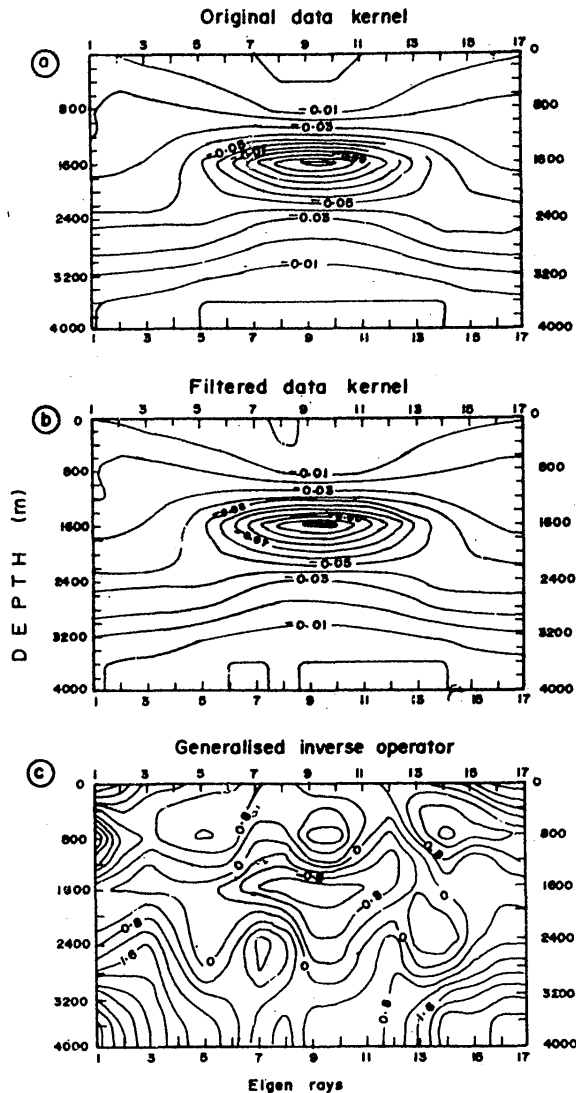


Fig. 6—(a) Original data kernel (A); (b) data kernel ($U_p \Gamma_p V_p^T$) maps constructed by combining in sequence (1 to 5) energetic modes; (c) generalized inverse ($V_p \Gamma_p^{-1} U_p^T$) maps constructed by combining in sequence (1 to 5) energetic modes

Influence of drifts—To study the influence of the source-receiver drifts (horizontal or vertical or both) on model parameters through travel time error in different rays, two cases of (a) assumed horizontal drift of 5 m and (b) assumed vertical drift of 2 m have been considered. The results presented in Table 1 show the magnitude of error resulting in the model parameter estimation. For example, if case (a) exists, the error in the model parameter will be of the order of 0.004 m/sec while if case (b) prevails the error in the model parameter

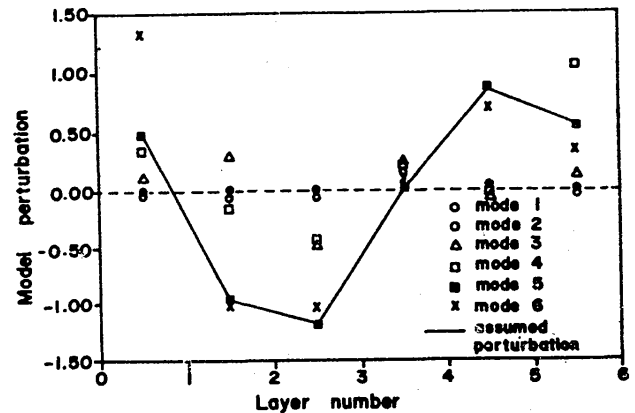


Fig. 7—Comparison of assumed and reconstructed sound speed perturbations

in different layers vary between 0.005 to 0.010 m/sec.

To make the inverse solution complete, the model and data resolution matrices are analysed¹⁰. The diagonal elements (Table 2a) for factors 1 through 6 of model resolution ($V V^T$) depict how well the individual model parameters are resolved. Any value less than unity indicates less resolution while unit value corresponds to good resolution. There are seventeen data measurements along the eigen rays and six model parameters associated with six layers. This system leads to poor resolution with less than five factors while a perfect resolution is seen for the five factors. By introducing the sixth factor, a perfect resolution is expected. But however, it leads to the deterioration of resolution as the noise also got amplified with the signal. This is due to the influence of a small positive eigen value in the activated space which increases its rank instead of increasing the dimension of the null space. It is noted that in layer four, the model parameter is nearly uniquely determined even for factor 2 (Table 2). The model parameter associated with surface layer is well resolved for $k=6$. Layers 2 to 5 are fairly resolved for factors $r=3, 4$ and 5.

The diagonal elements of $U U^T$ are shown in Table 3 for factors 1, 2, ..., 6. A value of unity indicates contribution of information independent of the other observations. Among all the rays, the most independent information is contained by 4.88° ray. This table, therefore, enables one to infer which of the rays present poor information resolution (resulting from sampling nearly the

Table 1—Results of six layer numerical experiment

Tomographic layers (m)	Sound speed		Anomaly-predicted minus assumed (m/sec)	Energetic modes			Source drift horizontal and vertical (m/sec)		Receiver drift horizontal and vertical (m/sec)	
	Predicted (m/sec)	Assumed (m/sec)		4 modes	5 modes	6 modes				
0- 400	1508.32	1507.84	0.48	0.35	0.49	1.32	0.0	0.0	0.0	0.0
400- 800	1500.75	1501.72	-0.97	-0.16	-0.91	-1.01				
800-1200	1497.55	1498.73	-1.18	-0.43	-1.18	-1.03				
1200-2000	1494.86	1494.77	0.09	0.18	0.07	0.09				
2000-3000	1503.35	1502.50	0.85	0.02	0.86	0.69				
3000-4000	1523.60	1523.04	0.56	1.04	0.57	0.34				
				0.35	0.49	1.33	0.0	0.0	0.0	2.0
				-0.16	-0.97	-1.01				
				-0.43	-1.18	-1.03				
				0.18	0.07	0.09				
				0.02	0.85	0.69				
				1.04	0.57	0.34				

Table 2—Model parameter resolution in each of layers for a factor r=1 through 6

Layer no.	Mode no.					
	1	2	3	4	5	6
1	0.001	0.016	0.068	0.118	0.128	1.000
2	0.015	0.174	0.519	0.696	0.998	1.000
3	0.033	0.173	0.714	0.714	0.972	1.000
4	0.785	0.992	0.993	0.994	0.999	1.000
5	0.165	0.638	0.638	0.643	0.965	1.000
6	0.001	0.008	0.068	0.835	0.938	1.000

Table 3—Information data resolution for each of seventeen eigen rays for factor r=1 through 6

Ray no.	Mode no.					
	1	2	3	4	5	6
1	0.018	0.058	0.102	0.461	0.482	0.485
2	0.028	0.095	0.107	0.115	0.131	0.293
3	0.026	0.095	0.126	0.148	0.148	0.299
4	0.029	0.098	0.122	0.211	0.328	0.441
5	0.041	0.072	0.517	0.523	0.599	0.635
6	0.059	0.066	0.215	0.219	0.223	0.223
7	0.108	0.132	0.140	0.140	0.280	0.335
8	0.127	0.213	0.223	0.224	0.224	0.224
9	0.145	0.312	0.323	0.326	0.439	0.490
10	0.131	0.232	0.242	0.243	0.249	0.253
11	0.090	0.094	0.096	0.097	0.224	0.273
12	0.060	0.066	0.205	0.209	0.214	0.215
13	0.036	0.100	0.105	0.120	0.123	0.240
14	0.029	0.096	0.118	0.202	0.313	0.423
15	0.026	0.094	0.124	0.145	0.145	0.284
16	0.030	0.120	0.131	0.133	0.367	0.371
17	0.018	0.057	0.102	0.485	0.511	0.516

same ocean region) as seen from the values in the boxes.

Following the analysis of the model and data resolutions, the present study indicates that the partial information contained in the data space is adequate to reconstruct the model parameters which is a case of overdeterminacy and reveals the usefulness of natural generalized inverse in the least square sense¹¹.

Acknowledgement

The authors are grateful to Dr. E. Desa, Director, for his keen interest in this study and to the Department of Ocean Development, Government of India, New Delhi for financial support.

References

- 1 Munk W H & Wunsch C, *Deep-Sea Res*, 26(A), (1979), 123.
- 2 Cornuelle B D, *Inverse methods and results from the 1981 Ocean Acoustic Tomography experiment*, Ph.D. thesis, Massachusetts Institute of Technology/Woods Hole Oceanographic Institution, USA, 1983.
- 3 Mahadevan R, Somayajulu Y K, Ramana Murty T V, Murty C S & Sastry J S, *Tomographic forward problem: Computational details for preparation of data kernel*, TR-NIO/7-89 (National Institute of Oceanography, Dona Paula, Goa, India), 1989, pp. 30.
- 4 Ramana Murty T V, Somayajulu Y K, Mahadevan R, Murty C S & Sastry J S, *Def Sci J*, 42 (1992) 69.
- 5 Lanczos C, *Linear differential operators*, (Van Nostrand, Reinhold, New York), 1961, pp. 564.
- 6 Jackson D D, *Geophys J Roy Astron Soc*, 28 (1982) 97.
- 7 Colburn J G, *Sound speed distribution in the western Indian Ocean*, TP-NUC/502, (Naval Undersea Centre, San Diego, California, USA), 1976, pp. 168.
- 8 Chen C -T & Millero F J, *J Acoust Soc Am*, 62 (1977) 1129.
- 9 Preisendorfer R W, Zwiers F W & Barnett T P, *Foundation of principal component selection rules*, SIO Ref. Ser. 81-4, (Scripps Institute of Oceanography, University of California, La Jolla) 1981, 192.
- 10 Chester D B, Rizzoli P M, De Ferrari H, *J Geophys Res*, 96, C4 (1991) 7023.
- 11 Menke W, *Geophysical data analysis: Discrete inverse theory*, (Academic Press Inc., New York), 1984, pp. 266.